

Chapter 30

ARM and Satellite Cloud Validation

ROGER MARCHAND

Department of Atmospheric Sciences, University of Washington, Seattle, Washington

1. Introduction

Many of the same factors that helped create the ARM Program, including the need to better constrain climate models, also helped lead to an expansion of Earth observing satellites in recent decades. In particular, starting in the late 1990s the National Aeronautics and Space Administration (NASA) Earth Observing System (EOS) program (Kaufman et al. 1998) began launching a series of polar-orbiting and low-inclination satellites for long-term global observations of the land surface, biosphere, atmosphere, and oceans.¹ Several of these missions had, and continue to have, a strong emphasis on clouds, aerosols, and radiation.

Among others, these missions included several large multi-instrument platforms, namely the Tropical Rainfall Measuring Mission (TRMM, launched November 1997), *Terra* (also known as *EOS-AM-1*, launched December 1999), and *Aqua* (*EOS-PM-1*, launched May 2002). All three of these large multi-instrument missions include measurements of broadband shortwave and longwave radiances from the Clouds and the Earth's Radiant Energy System (CERES) instruments, as well as multiple-wavelength narrow-band imagers—namely, the Visible and Infrared Scanner (VIRS) on board TRMM, the Multiangle Imaging Spectroradiometer (MISR) on board *Terra*, and the Moderate Resolution Imaging Spectroradiometer (MODIS) on board both *Terra* and

Aqua. A major advance of these new imagers is the improved calibration compared to previous generation observations due to the use of solar diffusers, a strong emphasis on vicarious calibration activities, and other factors. In combination with geostationary and polar-orbiting weather satellite observations, the CERES and NASA imager measurements have substantially improved knowledge of top-of-the-atmosphere radiative fluxes, including the variability of these fluxes and the large impact of clouds.

The MISR and MODIS imagers also make measurements at wavelengths not collected by weather satellites, at higher spatial resolutions (up to 250 m at some wavelengths), and in the case of MISR, at nine view angles along the satellite flight direction. These additional capabilities enable application of algorithms for the detection of clouds, as well as determination of their radiative or microphysical properties (such as the amount of water or ice) that were not previously possible. New does not necessarily mean better, and ARM played a pivotal role in characterizing or validating (as it is often called in the satellite community) retrievals of cloud properties from NASA EOS, NOAA weather (including geostationary), and other satellites.

Much of the ARM Program's role in satellite cloud retrieval validation stems from the program's dedication to developing and improving ground-based instruments, such as millimeter-wavelength cloud radar and Raman lidar, as well as the development of retrievals based on combinations of ground-based instruments including passive microwave radiometers and infrared interferometers (e.g., Shupe et al. 2008). Equally important has been the program's commitment to making measurements continuously at several sites (including tropical and high-latitude locations) over many years. These measurements have provided a large number of samples across a wide variety of meteorological conditions and enabled evaluation of satellite datasets with many differing orbits, as well as helping

¹ NASA's Earth Observing System Project Science Office: <http://eosps.gsf.nasa.gov/>.

Corresponding author address: Roger Marchand, Dept. of Atmospheric Sciences, University of Washington, 3737 Brooklyn Ave. NE, Seattle, WA 98105.
E-mail: rojmarch@u.washington.edu

to understand limitations in the diurnal sampling of non-geostationary sensors.

While not the focus of this chapter, the retrieval algorithms that ARM helped developed have not only provided validation data, but also helped in the development of radar, lidar, and combined instrument retrievals from space (e.g., Wang and Sassen 2002). In April 2006, NASA launched the *CloudSat* and *CALIPSO* missions, placing into orbit a millimeter-wavelength (W band, 95 GHz) cloud radar and dual-wavelength (532 and 1064 nm) lidar. In a process known as formation flying, these two platforms fly along nearly the same orbit as the *Aqua* platform, making observations separated by less than 2 min, and are controlled carefully so that the narrow radar and lidar beams gather data from overlapping ground points about 90% of the time. These three satellites, along with the NASA *Aura* and *Orbiting Carbon Observatory 2 (OCO-2)* satellites, the French *Polarization and Anisotropy of Reflectances for Atmospheric Sciences Coupled with Observations from a Lidar (PARASOL)* satellite, and the Japanese *Global Change Observation Mission–Water (GCOM-WI)*, form the satellite afternoon constellation or A-Train.²

In this chapter we summarize results from a variety of satellite cloud validation studies. Observations at the ARM sites have also made important contributions in validating surface and atmospheric properties such as surface radiation (e.g., Charlock and Alberta 1996), surface albedo (e.g., Jin et al. 2003; Trishchenko et al. 2008), microwave emissivity and soil moisture (e.g., Lin and Minnis 2000), precipitation (e.g., Sapiano and Arkin 2009), and water vapor (e.g., Tobin et al. 2006). However, here we focus on clouds since ARM has played a central role in validation of these quantities with few other programs providing as comprehensive a range of cloud observations and none with a longer cloud (millimeter wavelength) radar record. Our intent here is to provide representative examples of ARM contributions to satellite validation rather than trying to provide an exhaustive list. The examples focus on long-term measurements, but case study analyses have also provided important insights, especially for algorithm development.

2. Passive sensors and clouds

a. Cloud macrophysics: Cloud detection

In most satellite retrievals, the first step is to determine if a cloud is present; dividing the observed image into a set of image pixels that contain cloud (on which one might apply a retrieval for cloud microphysical or radiative properties, as

discussed later) and a set that are cloud free (on which one might apply surface and/or aerosol property retrievals). The cloud fraction (i.e., the number of cloudy pixels relative to total pixels) is perhaps the cloud property used most frequently in the evaluation of climate models. Thus, understanding how well and under what conditions clouds can be identified is critical.

Typically, the most difficult clouds to identify are optically thin high-altitude cirrus clouds and small-scale (often subimager resolution) cumulus clouds, because both of these cloud types may have only a small effect on observed visible and infrared images. That is, these clouds produce little contrast in the observed imagery between cloudy and cloud-free conditions, which means that the accuracy of satellite cloud detection schemes is dependent upon the underlying surface, making it important to have multiple validation sites.

At high latitudes, where the surface is often snow covered much of the year and the sun is low (near the horizon), cloud detection has traditionally been particularly challenging. This is because visibly bright snow-covered surfaces and shadowing by clouds greatly reduce the contrast between clouds and the surface at visible wavelengths, while cold surface temperatures with strong and frequent temperature inversions (colder air near the surface than above) complicate the use of infrared channels. In response to this challenge, cloud detection techniques have been developed combining observations at several infrared and shortwave-infrared wavelengths (the latter meaning wavelengths where both thermal emission and solar scattering contribute significantly). In particular, several wavelengths (or bands) were included in the MODIS instrument to improve surface retrievals and improve discrimination of cloud over snow and sea ice (Schueler and Barnes 1998).

Observations collected by the ARM Program at its North Slope of Alaska (NSA) sites at Barrow and Atkasuk, Alaska, have been used by several researchers to evaluate satellite cloud detection. For example, Berendes et al. (2004) compared MODIS (MOD35 product, collection 4) cloud detection with several ARM datasets including the ARM Active Remote Sensing of Cloud Layers (ARSCL) product, which combines data from the ARM vertically pointing cloud radar and lidar systems (Clothiaux et al. 2000). Berendes et al. (2004) generated a scatterplot of MODIS cloud fraction calculated over a 15-km region surrounding the ARM Barrow site against cloud fraction calculated from ARSCL data collected within 15 min of the MODIS overpass (Fig. 30-1). The ARM radar and lidar systems used are vertically pointing instruments with a very narrow field of view. Thus, these instruments produce a vertically resolved time series (sometimes called a time–height plot) of clouds as they pass over the ARM site.

² Stephens et al. (2002); <http://atrain.nasa.gov/intro.php>.

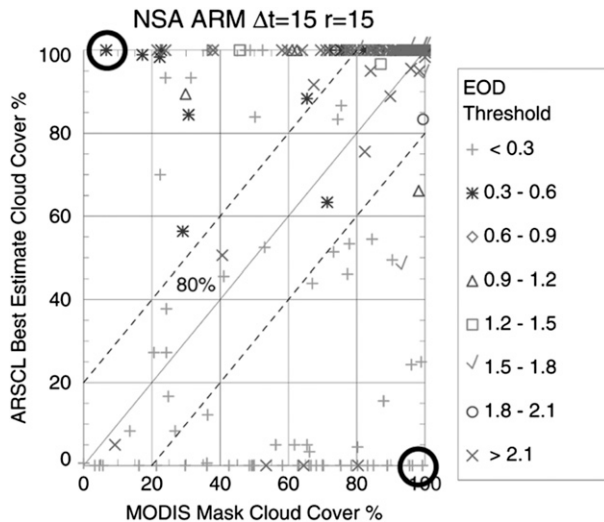


FIG. 30-1. Comparison of MODIS (MOD35 collection 4) cloud detection with ARM ARSCL (radar-lidar) product for the Barrow site. Symbols represent different optical depth (EOD) categories. Daytime data only. Taken from Berendes et al. (2004). Black circles denote cases examined in greater detail by Berendes et al. that are not discussed here.

In this figure, the symbols show an estimate for the cloud optical depth (a measure of how much direct sunlight is reflected or absorbed by the cloud before it reaches the surface). Small values of optical depth (less than 2) imply an optically thin cloud through which you could easily see the solar disk. These authors found agreement between the individual MODIS and ARSCL cloud fractions to better than 20%, more than 80% of the time. When the two datasets disagree, the cloud was typically either a broken low cloud over snow (asterisks in Fig. 30-1, which had a 15-min mean optical depth typically less than about 0.6) that was not detected by MODIS or optically thin high-altitude cirrus (with an optical depth less than about 0.3) that was in some cases not detected by the low-power micropulse lidar used in this study and in other cases not detected by MODIS.

This impressive level of cloud detection accuracy is similar to that found at other sites using MODIS, including at the ARM Southern Great Plains (SGP) site, where Ackerman et al. (2008) found agreement was approximately 85% between MODIS and the ARSCL in identifying cloud and clear scenes. In their approach, Ackerman et al. limited themselves to those cases that were identified by ARSCL over a 5-min window to be either cloudy at least 95% of the time (which were taken to be cloudy), or cloudy less than 5% of the time (which were taken to be clear). This analysis likewise identified thin cirrus as a primary driver of differences in cloud detection between MODIS and ground-based lidar systems. Ackerman et al. (2008) found that when the Arctic

High-Spectral Resolution Lidar detected a cloud and MODIS indicated clear, more than 60% of the time the optical depth (estimated from the lidar data) was less than 0.2 and 90% of the time the optical depth was less than 0.4. This is similar to what Marchand et al. (2007) found with MISR cloud detection using lidar observations from the ARM Barrow, SGP, and Nauru sites (see Fig. 30-2).

It is worth noting that the analysis of Berendes et al. (2004) was restricted to daytime conditions. Liu et al. (2004) found similarly good agreement in daytime cloud detection by MODIS (collection 4) but also that MODIS failed to detect more than 40% of the nighttime cloud cover over the ARM sites. Based on ARM and other ground-based datasets, Liu et al. were able to develop additional cloud tests (primarily utilizing the MODIS 7.2- μm water vapor and 14.2- μm carbon dioxide bands) reducing the misidentification of cloud from about 40% to 16% at the ARM sites at night. These tests were included subsequently in the next version of MODIS processing (collection 5).

b. Cloud macrophysics: Cloud-top height (CTH)

A climatically critical cloud property that satellites are in a particularly advantageous position to monitor is cloud-top height. As with cloud detection, the ARM ARSCL datasets have been extremely helpful in characterizing the accuracy of satellite imager and sounder retrievals of cloud-top height (or equivalently, cloud-top pressure) owing to the unambiguous range-resolved nature of the cloud radar and lidar observations. The ARM radars and lidars have typically operated with a range resolution of 90 m or better. This includes analysis of retrievals from many satellite imagers (e.g., Hollars et al. 2004; Smith et al. 2008; Mace et al. 2006, 2011), including the NASA MODIS and MISR imagers (e.g., Naud et al. 2002, 2005; Mace et al. 2005; Marchand et al. 2007), as well as infrared sounders (e.g., Hawkinson et al. 2005; Kahn et al. 2007). A detailed discussion of the various satellite retrieval techniques is beyond the scope of what can be included here and so we refer interested readers to the recent review article by Marchand et al. (2010) for a detailed description of the retrieval approaches and their errors for imagers.

Broadly, these analyses have found that, for *high-altitude clouds*, imager or sounder-based retrievals of cloud-top height tend to be located below “true” cloud top as detected by sensitive lidar systems. That is, many high-altitude clouds do not have a sharp upper boundary but rather have low amounts of condensate near cloud top (with low or modest values of optical extinction near cloud top). In this situation, the cloud top identified by imagers represents a “radiative-effective cloud top.” The exact position of this radiative-effective level varies

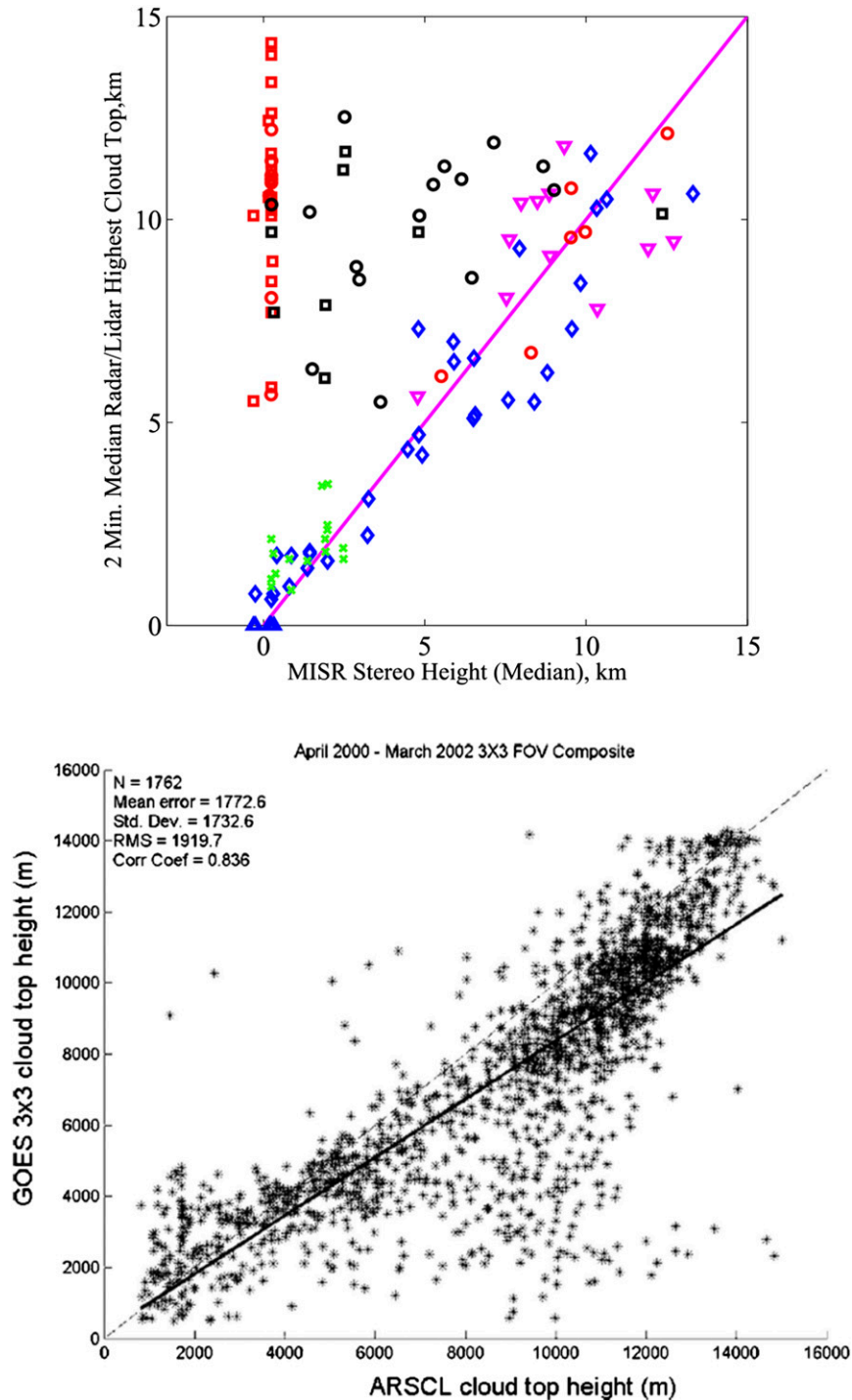


FIG. 30-2. Two comparisons of ARM radar–lidar and satellite-retrieved cloud-top height at SGP site. (top) MISR stereo-imaging retrieval [taken from [Marchand et al. \(2007\)](#)]. (bottom) GOES sounder CO₂ slicing retrieval [taken from [Hawkinson et al. \(2005\)](#)]. Symbols in (top) represent different cloud types. Red symbols are for very optically thin clouds (ARM retrieved optical depth < ~0.3), which MISR usually fails to detect. Black symbols are multilayer clouds, where the upper-level cloud is optically thin (ARM-retrieved optical depth < 1–2) and MISR has returned the height of a lower cloud layer. Other symbols represent various types of optically thick clouds. Blue is stratiform cloud (fills 11-km patch), green is broken boundary layer cloud, and magenta is cloud with diffuse (low condensate) cloud top. Uncertainty is higher at high altitudes (RMS ~ 1 km) than at lower altitudes (~500 m).

with the details of the retrievals and the vertical profile of cloud extinction. For vertically extensive clouds, it tends to be located within the cloud, often a kilometer below lidar cloud top.

For clouds with high values of optical extinction near cloud top, which includes most clouds with liquid water at the top, retrievals of cloud-top height are in reasonably good agreement with ARM radar and lidar datasets, with little bias and uncertainties (RMS errors) typically between 500 m and 1 km. One notable exception is that infrared-temperature techniques applied to boundary layer clouds under strong temperature inversions (typical in stratocumulus clouds) are often biased, placing cloud much too high in altitude. Figure 30-2 shows results taken from Marchand et al. (2007) and Hawkinson et al. (2005) comparing the MISR stereo-height algorithm and GOES sounder (CO₂ slicing technique) with ARM ARSCL. For the MISR example, red symbols are clouds that are too thin to be detected, while black symbols represent multilayer clouds with a thin upper-level cloud that MISR does not detect, and instead finds the altitude of a lower-altitude cloud layer.

Multilayer clouds present a major challenge to retrievals from imagers and are associated frequently with larger errors (Marchand et al. 2010). Algorithms specifically designed to detect multilayer clouds remain a topic of active research, and ARM datasets have been and will continue to be used in the evaluation of these algorithms (e.g., Baum et al. 2003; Chang and Li 2005; Minnis et al. 2007).

c. Cloud microphysics and optical properties

As discussed in Shupe et al. (2016, chapter 19), the development of retrievals based on radar and lidar data for cloud microphysical properties (principally cloud water content and effective particle size) and optical properties (principally optical depth) has been a topic of intensive research within the ARM community. Like satellite retrievals, ground-based retrievals make many simplifying assumptions and have their own characteristic errors, which must be considered carefully in any comparisons. Nonetheless, the ground-based observations often have finer vertical resolution and better sensitivity, because they have the advantage of being much closer to the object of study. ARM retrievals are also usually based on a combination of measurements from different sensors, and in particular, often include measurements of downward shortwave or infrared radiation that provides information on the transmissivity of the clouds (i.e., an integral constraint on the total cloud optical depth). In situ data are often used directly to validate satellite and ground-based retrievals as part of case studies (e.g., Dong et al. 2002) or in the

specification of some retrieval parameters such as mixtures of cloud particle habits or shapes [see Nasiri et al. (2002)]. However, these datasets are fundamentally sparse and more difficult to match up with satellites than ground-based retrievals, which provide for much larger datasets and better overall statistical measures.

Two examples of satellite microphysical and optical property validation studies are provided by Mace et al. (2005) for high-altitude ice clouds and Dong et al. (2008) for low clouds.

Mace et al. (2005) use a combination of matchup points (direct comparison of results from two dozen cirrus with coincident measurements) and broader regional statistics (comparing data gathered over a longer period and a larger area but not coincident in time or space) for the ARM SGP region. In the direct comparison, wind-profiler data were used to identify coincident areas for matching the time–height data gathered by ARM with MODIS imagery, and clouds were required to cover this full area. Two separate satellite retrievals (one derived from MODIS data by the MODIS Atmospheres Team and one derived from MODIS data by the CERES Science Team) were compared with results from two ground-based properties retrievals. Overall, Mace et al. show that there is a positive correlation in the effective particle size, the optical thickness, and the ice water path (vertical sum of ice water content/density) between the various methods, although sometimes there are significant biases.

Figure 30-3 shows several comparisons made by Mace et al. between the MODIS team retrieval (known as MOD06) and results from one of the ARM retrievals (known as the Z-radiance technique). The top three panels show results from the individual matchup points and the bottom two panels show distributions from the statistical analysis. The top three panels of Fig. 30-3 demonstrate a reasonable correspondence between the MOD06 and Z-radiance results for effective radius and ice water path. Summary statistics for these comparisons are given by Mace et al. but are not discussed here. The uncertainty bars show spatial and temporal variability over the matchup box. The MOD06 optical depths are biased slightly high with respect to the Z-radiance results. Not shown, the statistical regional analysis further bears out this bias and shows that MOD06 underrepresents the amount of cirrus with optical depths less than 1.0 (especially less than 0.5). However, for clouds with optical depths between 1 and 3, the distribution of cloud particle size and ice water path is quite good, as shown in the bottom two panels.

Dong et al. (2008) compared MODIS (CERES Team) and ARM-based retrieval of stratus cloud microphysical properties for the SGP site. The ARM retrievals were

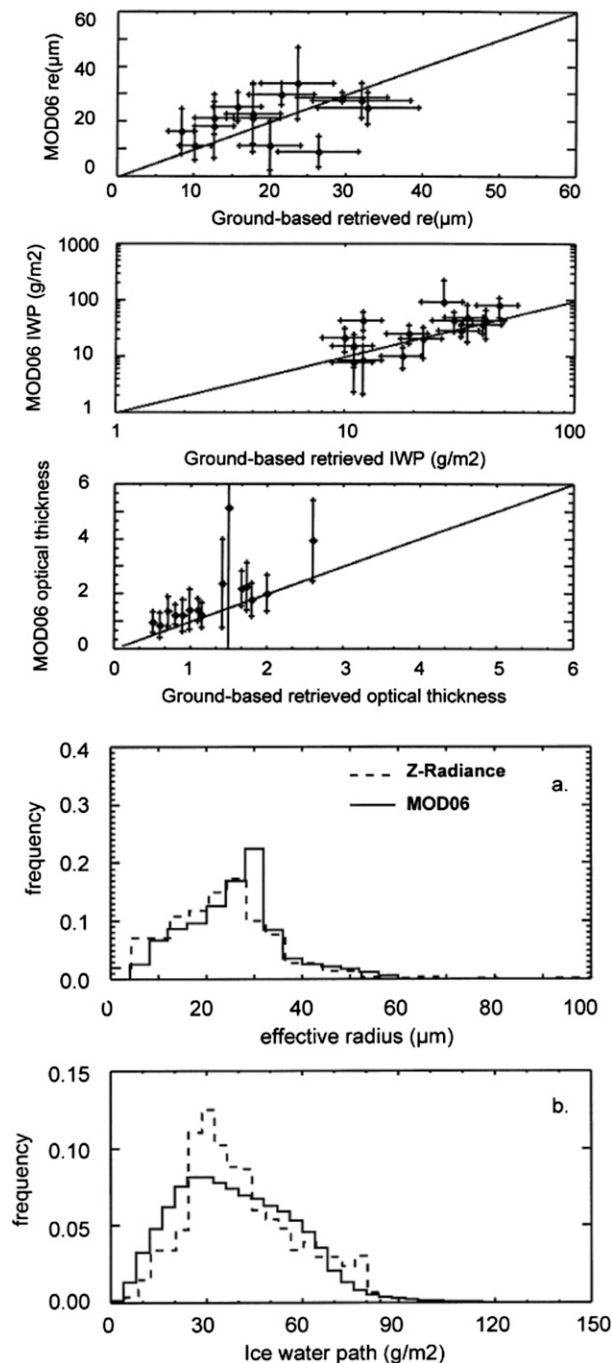


FIG. 30-3. (top three panels) Scatterplots of MOD06 (collection 4) vs Z-radiances microphysical retrievals for matchup points. (bottom two panels) The distributions of effective radius and ice water path for clouds with an optical depth between 1.0 and 3.0. MOD06 underrepresents clouds with an optical depth less than 1.0 (especially those with optical depth less than 0.5). Taken from Mace et al. (2005, see their Figs. 10 and 15).

based on a combination of ARM measurements from a pyranometer (downward hemispheric shortwave broadband surface flux), microwave radiometer, cloud radar, and micropulse lidar. For the period March 2000–December 2004, these authors identified 64 daytime cases with stratus clouds during the *Terra* overpass (~ 1030 local time) and 45 cases during the *Aqua* overpass (~ 1330 local time). These overpasses were further restricted to ensure clouds that were single layered with relatively large optical depths (ODs; $\text{OD} > 10$ for ARM retrieval, $\text{OD} > 5$ for MODIS), and unbroken (no clear satellite pixel within $30\text{ km} \times 30\text{ km}$ box and no gaps in ARM radar data over a 1-h period), reducing the number of matchup points to 33 and 21, respectively. Figure 30-4 shows scatterplots of microphysical properties for the *Terra* overpasses for this restricted set.

The differences (bias \pm standard deviation) between the *Terra* and ARM retrievals of effective radius, optical depth, and liquid water path for single-layer stratus are modest: $0.1 \pm 1.9\ \mu\text{m}$ ($1.2\% \pm 23.5\%$), 1.3 ± 9.5 ($-3.6\% \pm 26.2\%$), and $0.6 \pm 49.9\ \text{g m}^{-2}$ ($0.3\% \pm 27\%$), respectively, with percentages relative to the mean. The corresponding correlation coefficients are high for optical depth and liquid water path, 0.87 and 0.89, respectively, but relatively poor for effective radius at 0.44. Dong et al. suggest this poorer agreement in effective radius may be due the variability in the vertical profile of effective radius, which is not determined by the satellite retrievals. On the other hand, imager-based retrievals of effective radius are known to be sensitive to horizontal variability of cloud properties and this may be an issue even for stratocumulus clouds, which are relatively homogenous compared to cumulus and most other clouds (e.g., Marshak et al. 2006). The overall statistics for the *Aqua* overpasses (not shown), as well as when taken across all stratus cases (without stringent homogeneity conditions) are similar [see Table 4 in Dong et al. (2008)].

3. CloudSat, CALIPSO, and multi-instrument retrievals

The advent of space-borne cloud radar (*CloudSat*; Stephens et al. 2002) coupled with a two-wavelength lidar (*CALIPSO*; Winker et al. 2009) is providing an unprecedented look into the vertical structure of hydrometeor systems around the globe. As with the ARM radar and lidars that preceded them, these instruments have become a focus for the development of many macro and microphysical retrievals. The *CloudSat* and *CALIPSO* instruments do not scan, but collect data only along a very narrow swath or curtain as the satellites move along their orbits. This small sampling volume

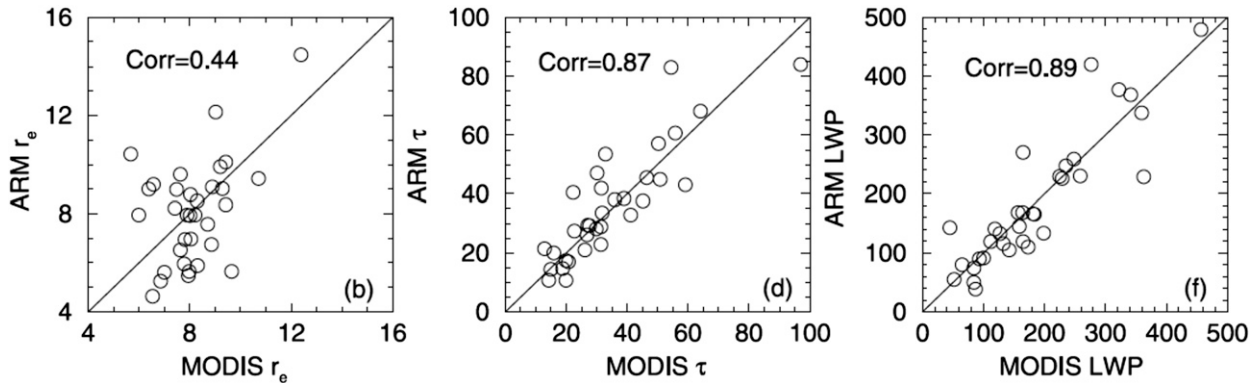


FIG. 30-4. Comparison of MODIS-retrieved (CERES Team) stratus properties and ARM retrieval over the SGP site. Taken from [Dong et al. \(2008\)](#), see their Fig. 5).

provides many fewer samples than satellite imagers, making comparison of these data with ground-based instruments more difficult. Nonetheless, statistical comparisons using several years of observations have been published recently.

Direct comparison of *CloudSat* cloud fractions and reflectivity distributions for nonprecipitating clouds show good agreement with both ARM radars and airborne radars ([Liu et al. 2010](#); [Protat et al. 2009](#)), while comparison of ARM and *CALIPSO* lidar have produced valuable insights into the detection capabilities of these systems for very optically thin tropical cirrus ([Thorsen et al. 2013](#)). With regard to cloud radar, precipitating systems cause considerable attenuation of the ARM cloud radars due to water on the radome and for both systems within the atmosphere, making comparisons in precipitating conditions problematic.

[Figure 30-5](#) shows a comparison of ARM and *CloudSat*-derived cloud occurrence with height (top panel) and measured reflectivity distribution collected at all altitudes above 1 km (bottom panel) for non- or lightly precipitating clouds. ARM data are shown in black and *CloudSat* data are shown as a white line with uncertainty bars (due to sampling) depicted with gray shading. Uncertainties due to sampling by the ARM system are very small (not shown) due to the abundant observations a fixed site provides. This figure shows a high degree of correspondence, with *CloudSat* detecting only slightly more low-reflectivity clouds, primarily at high altitudes. This additional cloud is due in part to lower resolution of the *CloudSat* radar (cf. vertical ~ 480 m and horizontal ~ 2 km for *CloudSat* and ~ 90 m \times 10 s for ARM), which tends to make clouds look a bit larger than they are, and in part to attenuation suffered by the ARM system.

Evaluation of microphysical retrievals based on *CloudSat* and *CALIPSO* measurements is an area of

ongoing research. [Protat et al. \(2010, 2011\)](#) published a comparison of radar–lidar retrievals using ARM observations of tropical ice clouds at Darwin, Australia, with the two most basic *CloudSat* operational retrievals, known as the radar-only product (2B-CWC-RO) and the radar optical depth product (2B-CWC-RVOD).

[Figure 30-6](#) compares distributions of retrieved ice water content, extinction, effective radius, and cloud particle number concentration between the *CloudSat* radar-only (RO) retrieval, ground-based radar–lidar (gray line), and simple ground-based radar temperature approach (dashed line) for ice-only clouds at the ARM Darwin site. The *CloudSat* radar-only retrieval uses only the measured cloud reflectivity, and so might not be expected to produce very accurate results compared with multi-instrument retrievals. Nonetheless, the distribution of *CloudSat* radar-only retrieved ice water content (top-left panel) is in remarkably good agreement. However, it is worth noting that this distribution includes clouds at altitudes ranging from 5 to 16 km above the surface. While the distribution aggregated from data at all altitudes compares favorably, there is a clear overestimation of ice water contents above 12 km and an underestimation of ice water contents below 10 km, which is discussed by [Protat et al. \(2010\)](#) and not shown here. Perhaps not surprisingly, the *CloudSat* radar-only effective radius and number concentration retrievals appear to have significant biases. [Protat et al. \(2010\)](#) indicate that errors in cloud microphysics using the radar optical depth (RVOD) retrieval are similar to those shown here for the radar-only retrieval. Of course, multiple-instrument retrievals have been developed for *CloudSat*, and ARM will no doubt be involved in evaluating these products in the future, as well as to examine the impact of diurnal variability, which is not observed by *CloudSat* and other sun-synchronous satellites.

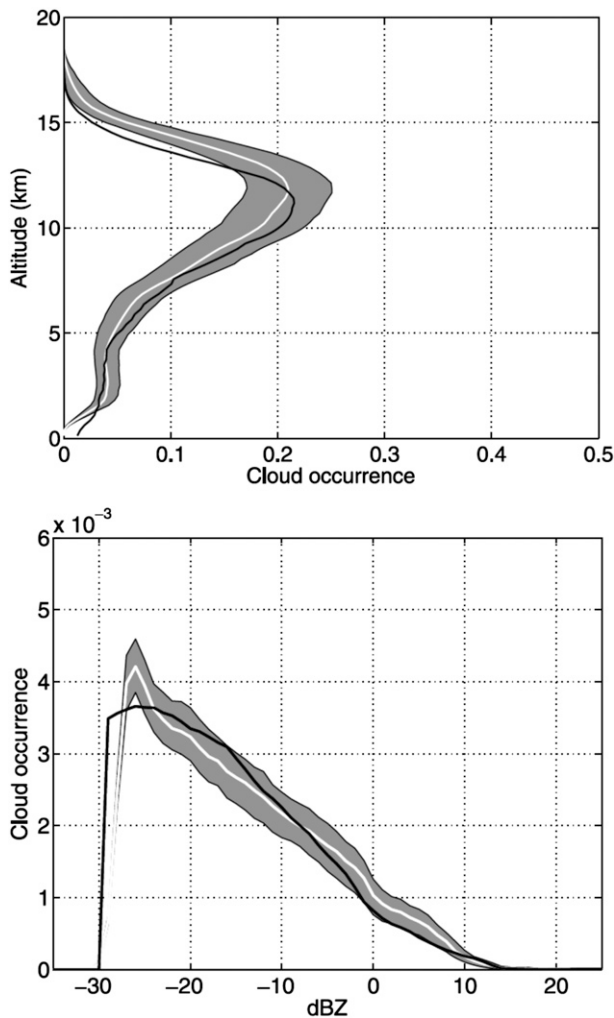


FIG. 30-5. Comparison of ARM 35-GHz cloud radar with *CloudSat* 95-GHz systems for nonprecipitating clouds using *CloudSat* data collected within 4° of the ARM site in Darwin, Australia. (top) The occurrence of clouds with reflectivity greater than -30 dBZ (cloud fraction with height) and (bottom) the distribution of reflectivity at all altitudes. Taken from Liu et al. (2010).

4. Discussion and outlook

In summary, ARM has played a key role in the validation of satellite cloud detection schemes, as well as satellite retrievals of cloud-top height, microphysical, and optical properties, and examples of each of these activities were provided. While the examples shown here focused largely on NASA Earth observing satellites, specifically MODIS, MISR, and *CloudSat*, these examples represent only a small subset of the cloud validation research that has been undertaken. ARM data have been used in the evaluation of retrievals from many other satellites including those on geostationary (e.g., Dong et al. 2002; Hollars et al.

2004; Smith et al. 2008), as well as European platforms (e.g., Riedi et al. 2001; Vanbauce et al. 2003; Larar et al. 2009).

It is not coincidental that the examples shown here have focused largely on horizontally extensive stratus and cirrus clouds. In part, this is because horizontally uniform clouds reduce difficulties (variability) associated with trying to match the nearly instantaneous and typically lower-resolution satellite datasets with the time–height data produced by the nadir-pointing radar and lidar systems that ARM began deploying in 1996. Comparisons of satellite datasets with broken or otherwise less homogenous clouds generally show larger differences including significant biases, especially for microphysical and optical quantities such as cloud optical depth. These differences may well be due to effects of “subpixel” or unresolved variability in cloud properties. Retrievals nearly universally assume constant cloud properties over whatever resolution the observations are taken (e.g., Mace et al. 2011). However, both satellite and ground-based retrievals are also expected to be of lower quality and in some cases are known to have significant biases for clouds that are spatially inhomogeneous even at resolved scales (especially near cloud edges) owing to the widespread use of one-dimensional radiative transfer in modeling cloud reflectivity or transmissivity at all wavelengths. Variability of cloud properties also complicates validation of retrievals against in situ data, making direct assessment of errors due to spatial variability difficult.

The ARM Program is currently in the process of deploying scanning dual-polarization multiple-wavelength cloud radars (K- and W- or K- and X-band systems) at all of its fixed and mobile sites (Mather and Voyles 2013). These scanning systems will lead to the development of new retrievals that will capture spatial variability at scales resolved by the radars. In addition to providing improved retrievals and enabling more effective evaluations against in situ measurements, the scanning radars are expected to provide insights into the effects of spatial variability on established (vertically pointing) algorithms.

It is also not coincidental that the examples discussed in this chapter avoided precipitating systems. While there has been some research into retrieving rain rates and other microphysical quantities from ARM vertically pointing radars (e.g., Matrosov et al. 2006), surface precipitation corrupts observations from many ARM instruments and the program has naturally focused on nonprecipitating conditions. The ARM Program is also in the process of deploying a variety of scanning polarimetric precipitation radars (C- and

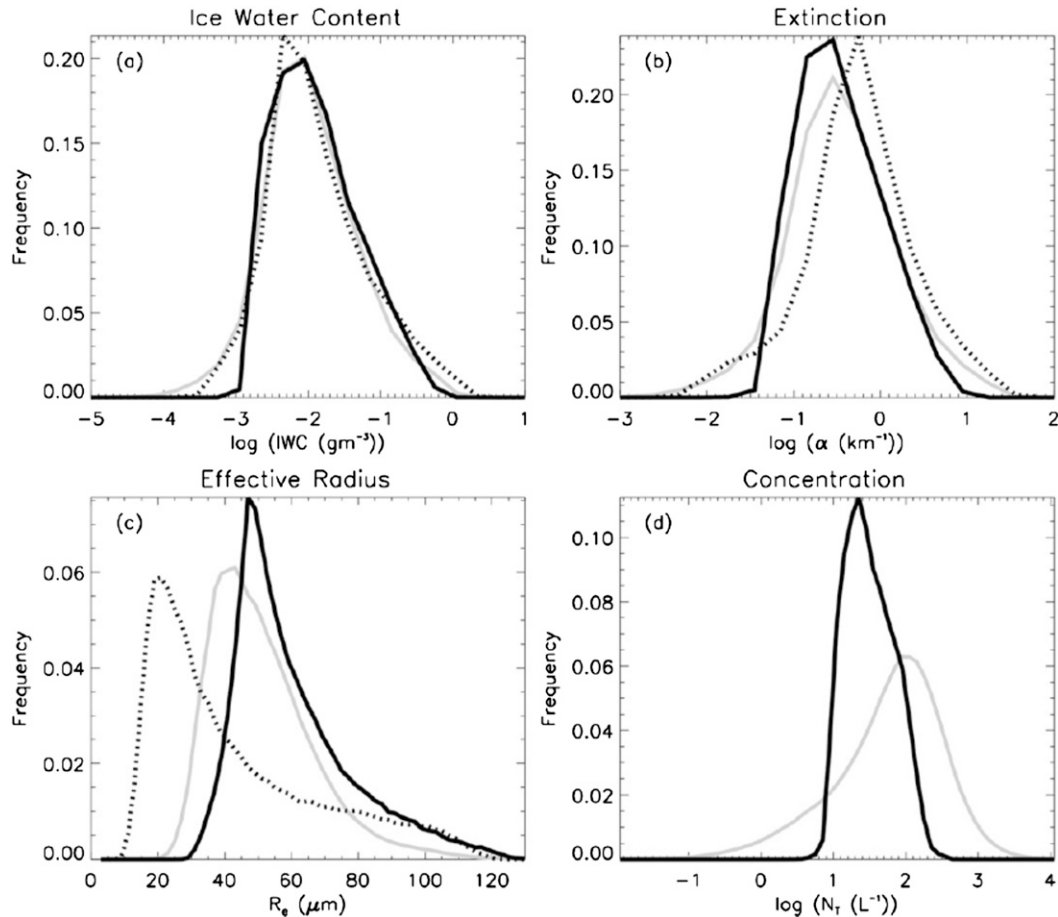


FIG. 30-6. Comparison of *CloudSat* radar-only product (solid line) with ground-based radar-lidar (gray line) and simple ground-based radar temperature approach (dashed line) for ice-only clouds at the ARM Darwin site. Taken from Protat et al. (2010).

X-band systems). The combination of scanning precipitation and cloud radar systems will no doubt lead to further advancements in combined cloud and precipitation microphysical retrievals and a future role for the ARM Program in the validation of satellite-based precipitation retrievals, such as those from the NASA Global Precipitation Measurement (GPM) mission. ARM data gathered during the recent ARM Mid-latitude Convective Continental Clouds Experiment (M3CE) in combination with NASA aircraft data were used in the development of GPM algorithms before launch of this satellite in 2014 (e.g., Petersen and Jensen 2011). With regard to cloud properties, it is hoped that the combination of cloud radar with polarimetric C- and X-band data will provide constraints on ice crystal habit, which is a source of great uncertainty in both ground-based and satellite retrievals (McFarlane and Marchand 2008) and help constrain retrievals in mixed-phase clouds, which remain rudimentary except perhaps for thin Arctic stratus.

While the presence of *CALIPSO* and *CloudSat* (cloud radar and lidar in space) and the global perspective these data bring have to some degree reduced the importance of ARM radar and lidar data for cloud validation, these sensors are approaching the end of their mission lives and ARM still has much to contribute to future satellite validation. In addition to advances that will likely come from scanning radar discussed above, the complete diurnal sampling provided by ARM is critical to evaluating the representativeness of retrievals from polar-orbiting sensors (including future radar and lidar missions such as EarthCARE)³, and will be of great value in the direct evaluation of the next generation of geostationary weather satellites, GOES-R.⁴

³ Bezy et al. (2005); http://www.esa.int/Our_Activities/Observing_the_Earth/The_Living_Planet_Programme/Earth_Explorers/EarthCARE.

⁴ Schmit et al. (2005); <http://www.goes-r.gov/>.

REFERENCES

- Ackerman, S. A., R. E. Holz, R. Frey, E. W. Eloranta, B. C. Maddux, and M. McGill, 2008: Cloud detection with MODIS. Part II: Validation. *J. Atmos. Oceanic Technol.*, **25**, 1073–1086, doi:10.1175/2007JTECHA1053.1.
- Baum, B. A., R. A. Frey, G. G. Mace, M. K. Harkey, and P. Yang, 2003: Nighttime multilayered cloud detection using MODIS and ARM data. *J. Appl. Meteor.*, **42**, 905–919, doi:10.1175/1520-0450(2003)042<0905:NMCDUM>2.0.CO;2.
- Berendes, T. A., D. A. Berendes, R. M. Welch, E. G. Dutton, T. Uttal, and E. E. Clothiaux, 2004: Cloud cover comparisons of the MODIS daytime cloud mask with surface instruments at the north slope of Alaska ARM site. *IEEE Trans. Geosci. Remote Sens.*, **42**, 2584–2593, doi:10.1109/TGRS.2004.835226.
- Bezy, J.-L., W. Leibbrandt, A. Heliere, P. Silvestrin, C.-C. Lin, P. Ingmann, T. Kimura, and H. Kumagai, 2005: The ESA Earth Explorer EarthCARE mission. *Earth Observing Systems X*, J. J. Butler, Ed., International Society for Optical Engineering (SPIE Proceedings, Vol. 5882), doi:10.1117/12.619438.
- Chang, F., and Z. Li, 2005: A new method for detection of cirrus overlapping water clouds and determination of their optical properties. *J. Atmos. Sci.*, **62**, 3993–4009, doi:10.1175/JAS3578.1.
- Charlock, T. P., and T. L. Alberta, 1996: The CERES/ARM/GEWEX Experiment (CAGEX) for the retrieval of radiative fluxes with satellite data. *Bull. Amer. Meteor. Soc.*, **77**, 2673–2683, doi:10.1175/1520-0477(1996)077<2673:TCEFTR>2.0.CO;2.
- Clothiaux, E. E., T. P. Ackerman, G. G. Mace, K. P. Moran, R. T. Marchand, M. A. Miller, and B. E. Martner, 2000: Objective determination of cloud heights and radar reflectivities using a combination of active remote sensors at the ARM CART sites. *J. Appl. Meteor.*, **39**, 645–665, doi:10.1175/1520-0450(2000)039<0645:ODOCHA>2.0.CO;2.
- Dong, X., G. Mace, P. Minnis, W. L. Smith, M. Poellot, R. T. Marchand, and A. D. Rapp, 2002: Comparison of stratus cloud properties deduced from surface, GOES, and aircraft data during the March 2000 ARM Cloud IOP. *J. Atmos. Sci.*, **59**, 3265–3284, doi:10.1175/1520-0469(2002)059<3265:COCPD>2.0.CO;2.
- , P. Minnis, B. Xi, S. Sun-Mack, and Y. Chen, 2008: Comparison of CERES-MODIS stratus cloud properties with ground-based measurements at the DOE ARM Southern Great Plains site. *J. Geophys. Res.*, **113**, D03204, doi:10.1029/2007JD008438.
- Hawkinson, J. A., W. Feltz, and S. A. Ackerman, 2005: A comparison of GOES sounder- and cloud lidar- and radar-retrieved cloud-top heights. *J. Appl. Meteor.*, **44**, 1234–1242, doi:10.1175/JAM2269.1.
- Hollars, S., Q. Fu, J. Comstock, and T. Ackerman, 2004: Comparison of cloud-top height retrievals from ground-based 35 GHz MMCR and GMS-5 satellite observations at ARM TWP Manus site. *Atmos. Res.*, **72**, 169–186, doi:10.1016/j.atmosres.2004.03.015.
- Jin, Y., C. B. Schaaf, C. E. Woodstock, F. Gao, X. Li, A. H. Strahler, W. Lucht, and S. Liang, 2003: Consistency of MODIS surface bidirectional reflectance distribution function and albedo retrievals: 2. Validation. *J. Geophys. Res.*, **108**, 4159, doi:10.1029/2002JD002804.
- Kahn, B. H., A. Eldering, A. J. Braverman, E. J. Fetzer, J. H. Jiang, E. Fishbein, and D. L. Wu, 2007: Toward the characterization of upper tropospheric clouds using Atmospheric Infrared Sounder and Microwave Limb Sounder observations. *J. Geophys. Res.*, **112**, D05202, doi:10.1029/2006JD007336.
- Kaufman, Y. J., D. D. Herring, K. J. Ranson, and G. J. Collatz, 1998: Earth observing system AM1 mission to Earth. *IEEE Trans. Geosci. Remote Sens.*, **36**, 1045–1055, doi:10.1109/36.700989.
- Larar, A. M., W. L. Smith, D. K. Zhou, X. Liu, H. Revercomb, J. P. Taylor, S. M. Newman, and P. Schlüssel, 2009: IASI spectral radiance performance validation: Case study assessment from the JAIVEx field campaign. *Atmos. Chem. Phys. Discuss.*, **9**, 10 193–10 234, doi:10.5194/acpd-9-10193-2009.
- Lin, B., and P. Minnis, 2000: Temporal variations of land surface microwave emissivities over the Atmospheric Radiation Measurement Program Southern Great Plains site. *J. Appl. Meteor.*, **39**, 1103–1116, doi:10.1175/1520-0450(2000)039<1103:TVOLSM>2.0.CO;2.
- Liu, Y., J. R. Key, R. A. Frey, S. A. Ackerman, and W. P. Menzel, 2004: Nighttime polar cloud detection with MODIS. *Remote Sens. Environ.*, **92**, 181–194, doi:10.1016/j.rse.2004.06.004.
- Liu, Z., R. Marchand, and T. Ackerman, 2010: A comparison of observations in the tropical western Pacific from ground-based and satellite millimeter-wavelength cloud radars. *J. Geophys. Res.*, **115**, D24206, doi:10.1029/2009JD013575.
- Mace, G. G., Y. Zhang, S. Platnick, M. D. King, P. Minnis, and P. Yang, 2005: Evaluation of cirrus cloud properties derived from MODIS data using cloud properties derived from ground-based observations collected at the ARM SGP site. *J. Appl. Meteor.*, **44**, 221–240, doi:10.1175/JAM2193.1.
- , and Coauthors, 2006: Cloud radiative forcing at the Atmospheric Radiation Measurement Program Climate Research Facility: 1. Technique, validation, and comparison to satellite-derived diagnostic quantities. *J. Geophys. Res.*, **111**, D11S90, doi:10.1029/2005JD005921.
- , S. Houser, S. Benson, S. A. Klein, and Q. Min, 2011: Critical evaluation of the ISCCP simulator using ground-based remote sensing data. *J. Climate*, **24**, 1598–1612, doi:10.1175/2010JCLI3517.1.
- Marchand, R. T., T. P. Ackerman, and C. Moroney, 2007: An assessment of Multiangle Imaging Spectroradiometer (MISR) stereo-derived cloud top heights and cloud top winds using ground-based radar, lidar, and microwave radiometers. *J. Geophys. Res.*, **112**, D06204, doi:10.1029/2006JD007091.
- , —, M. Smyth, and W. B. Rossow, 2010: A review of cloud top height and optical depth histograms from MISR, ISCCP, and MODIS. *J. Geophys. Res.*, **115**, D16206, doi:10.1029/2009JD013422.
- Marshak, A., S. Platnick, T. Varnai, G. Wen, and R. F. Cahalan, 2006: Impact of three-dimensional radiative effects on satellite retrievals of cloud droplet sizes. *J. Geophys. Res.*, **111**, D09207, doi:10.1029/2005JD006686.
- Mather, J. H., and J. W. Voyles, 2013: The ARM Climate Research Facility: A review of structure and capabilities. *Bull. Amer. Meteor. Soc.*, **94**, 377–392, doi:10.1175/BAMS-D-11-00218.1.
- Matrosov, S. Y., P. T. May, and M. D. Shupe, 2006: Rainfall profiling using Atmospheric Radiation Measurement Program vertically pointing 8-mm wavelength radars. *J. Atmos. Oceanic Technol.*, **23**, 1478–1491, doi:10.1175/JTECH1957.1.
- McFarlane, S. A., and R. T. Marchand, 2008: Analysis of ice crystal habits derived from MISR and MODIS observations over the ARM Southern Great Plains site. *J. Geophys. Res.*, **113**, D07209, doi:10.1029/2007JD009191.

- Minnis, P., J. Huang, B. Lin, Y. Yi, R. F. Arduini, T.-F. Fan, J. K. Ayers, and G. G. Mace, 2007: Ice cloud properties in ice-over-water cloud systems using Tropical Rainfall Measuring Mission (TRMM) visible and infrared scanner and TRMM Microwave Imager data. *J. Geophys. Res.*, **112**, D06206, doi:[10.1029/2006JD007626](https://doi.org/10.1029/2006JD007626).
- Nasiri, S. L., B. A. Baum, A. J. Heymsfield, P. Yang, M. Poellot, D. P. Kratz, and Y. X. Hu, 2002: Development of midlatitude cirrus models for MODIS using FIRE-I, FIRE-II, and ARM in situ data. *J. Appl. Meteor.*, **41**, 197–217, doi:[10.1175/1520-0450\(2002\)041<0197:TDOMCM>2.0.CO;2](https://doi.org/10.1175/1520-0450(2002)041<0197:TDOMCM>2.0.CO;2).
- Naud, C. M., J.-P. Muller, and E. E. Clothiaux, 2002: Comparison of cloud top heights derived from MISR stereo and MODIS CO₂-slicing. *Geophys. Res. Lett.*, **29**, doi:[10.1029/2002GL015460](https://doi.org/10.1029/2002GL015460).
- , —, —, B. A. Baum, and W. P. Menzel, 2005: Intercomparison of multiple years of MODIS, MISR and radar cloud-top heights. *Ann. Geophys.*, **23**, 2415–2424, doi:[10.5194/angeo-23-2415-2005](https://doi.org/10.5194/angeo-23-2415-2005).
- Petersen, W. A., and M. P. Jensen, 2011: Physical validation of GPM retrieval algorithms over land: An overview of the Mid-Latitude Continental Convective Clouds Experiment (MC3E). *2011 Fall Meeting*, San Francisco, CA, Amer. Geophys. Union, Abstract H42E-01.
- Protat, A., and Coauthors, 2009: Assessment of Cloudsat reflectivity measurements and ice cloud properties using ground-based and airborne cloud radar observations. *J. Atmos. Oceanic Technol.*, **26**, 1717–1741, doi:[10.1175/2009JTECHA1246.1](https://doi.org/10.1175/2009JTECHA1246.1).
- , J. Delanoë, E. J. O'Connor, and T. S. L'Ecuyer, 2010: The evaluation of *CloudSat* and CALIPSO ice microphysical products using ground-based cloud radar and lidar observations. *J. Atmos. Oceanic Technol.*, **27**, 793–810, doi:[10.1175/2009JTECHA1397.1](https://doi.org/10.1175/2009JTECHA1397.1); Corrigendum, **28**, 734–735, doi:[10.1175/2010JTECHA1504.1](https://doi.org/10.1175/2010JTECHA1504.1).
- Riedi, J., P. Goloub, and R. T. Marchand, 2001: Comparison of POLDER cloud phase retrievals to active remote sensors measurements at the ARM SGP site. *Geophys. Res. Lett.*, **28**, 2185–2188, doi:[10.1029/2000GL012758](https://doi.org/10.1029/2000GL012758).
- Sapiano, M. R. P., and P. A. Arkin, 2009: An intercomparison and validation of high-resolution satellite precipitation estimates with 3-hourly gauge data. *J. Hydrometeorol.*, **10**, 149–166, doi:[10.1175/2008JHM1052.1](https://doi.org/10.1175/2008JHM1052.1).
- Schmit, T. J., M. M. Gunshor, W. P. Menzel, J. J. Gurka, J. Li, and A. S. Bachmeier, 2005: Introducing the next-generation advanced baseline imager on GOES-R. *Bull. Amer. Meteor. Soc.*, **86**, 1079–1096, doi:[10.1175/BAMS-86-8-1079](https://doi.org/10.1175/BAMS-86-8-1079).
- Schueler, C. F., and W. L. Barnes, 1998: Next-generation MODIS for Polar Operational Environmental Satellites. *J. Atmos. Oceanic Technol.*, **15**, 430–439, doi:[10.1175/1520-0426\(1998\)015<0430:NGMFPO>2.0.CO;2](https://doi.org/10.1175/1520-0426(1998)015<0430:NGMFPO>2.0.CO;2).
- Shupe, M. D., and Coauthors, 2008: A focus on mixed-phase clouds: The status of ground-based observational methods. *Bull. Amer. Meteor. Soc.*, **89**, 1549–1562, doi:[10.1175/2008BAMS2378.1](https://doi.org/10.1175/2008BAMS2378.1).
- , J. M. Comstock, D. D. Turner, and G. G. Mace, 2016: Cloud property retrievals in the ARM Program. *The Atmospheric Radiation Measurement (ARM) Program: The First 20 Years*, *Meteor. Monogr.*, No. 57, Amer. Meteor. Soc., doi:[10.1175/AMSMONOGRAPHS-D-15-0030.1](https://doi.org/10.1175/AMSMONOGRAPHS-D-15-0030.1).
- Smith, W. L., Jr., P. Minnis, H. Finney, R. Palikonda, and M. M. Khaiyer, 2008: An evaluation of operational GOES-derived single-layer cloud top heights with ARSCL data over the ARM Southern Great Plains site. *Geophys. Res. Lett.*, **35**, L13820, doi:[10.1029/2008GL034275](https://doi.org/10.1029/2008GL034275).
- Stephens, G. L., and Coauthors, 2002: The CloudSat mission and the A-Train: A new dimension of space-based observations of clouds and precipitation. *Bull. Amer. Meteor. Soc.*, **83**, 1771–1790, doi:[10.1175/BAMS-83-12-1771](https://doi.org/10.1175/BAMS-83-12-1771).
- Thorsen, T. J., Q. Fu, J. M. Comstock, C. Sivaraman, M. A. Vaughan, D. M. Winker, and D. D. Turner, 2013: Macrophysical properties of tropical cirrus clouds from the CALIPSO satellite and from ground-based micropulse and Raman lidars. *J. Geophys. Res. Atmos.*, **118**, 9209–9220, doi:[10.1002/jgrd.50691](https://doi.org/10.1002/jgrd.50691).
- Tobin, D. C., and Coauthors, 2006: Atmospheric Radiation Measurement site atmospheric state best estimates for Atmospheric Infrared Sounder temperature and water vapor retrieval validation. *J. Geophys. Res.*, **111**, D09S14, doi:[10.1029/2005JD006103](https://doi.org/10.1029/2005JD006103).
- Trishchenko, A. P., Y. Luo, K. V. Khlopenkov, and S. Wang, 2008: A method to derive the multispectral surface albedo consistent with MODIS from historical AVHRR and VGT satellite data. *J. Appl. Meteor. Climatol.*, **47**, 1199–1221, doi:[10.1175/2007JAMCI724.1](https://doi.org/10.1175/2007JAMCI724.1).
- Vanbauce, C., B. Cadet, and R. T. Marchand, 2003: Comparison of POLDER apparent and corrected oxygen pressure to ARM/MMCR cloud boundary pressures. *Geophys. Res. Lett.*, **30**, 1212, doi:[10.1029/2002GL016449](https://doi.org/10.1029/2002GL016449).
- Wang, Z., and K. Sassen, 2002: Cirrus cloud microphysical property retrieval using lidar and radar measurements. Part I: Algorithm description and comparison with in situ data. *J. Appl. Meteor.*, **41**, 218–229, doi:[10.1175/1520-0450\(2002\)041<0218:CCMPRU>2.0.CO;2](https://doi.org/10.1175/1520-0450(2002)041<0218:CCMPRU>2.0.CO;2).
- Winker, D. M., M. A. Vaughan, A. Omar, Y. Hu, K. A. Powell, Z. Liu, W. H. Hunt, and S. A. Young, 2009: Overview of the CALIPSO mission and CALIOP data processing algorithms. *J. Atmos. Oceanic Technol.*, **26**, 2310–2323, doi:[10.1175/2009JTECHA1281.1](https://doi.org/10.1175/2009JTECHA1281.1).